Conference Article

Multisim-Based Model for Unimorph Piezoelectric Energy Harvesters

Constantinos Tramantzas

Department of Electrical Engineering, Technological Educational Institute of Eastern Macedonia and Thrace Ag. Loukas, 65404 Kavala, Greece

_____

Abstract

Piezoelectric transduction has received great attention for vibration-to-electric energy conversion in the last years. Cantilevered beams with piezoelectric layers are lately more and more frequently used as energy harvesters. The development of piezoelectric energy harvesting systems needs accurate models for system behavior prediction and evaluation. In this paper, a Multisim-based distributed parameter model is proposed. In the modeling procedure, Euler-Bernoulli beam theory is used. A procedure for obtaining the model parameters is described.

Keywords*:* energy harvesting; vibration mode; electromechanical behavior; Multisim model.
_____

1 INTRODUCTION

The development of piezoelectric energy harvesting systems needs accurate models for system behavior prediction and evaluation. Different approaches for energy harvester modeling given in the literature sources, are based on the description of the physical processes in the active medium [1]. The typical design for piezoelectric EH for unimorph structures is based on the cantilever beam system [2] as vibrations are considered the main external mechanical force [3]. I used the Euler-Bernoulli and Rayleigh-Ritz solution to model the beam design. [4]. This modeling approach allows predicting the electromechanical response in higher vibration modes. However, since the utilized approximation technique is based on parameter discretization of a continuous distributed system, the solution is not exact. The used analytical modeling approach [5] is about a single vibration mode expression in the piezoelectric relation that generates so that it can connect the electric displacement in order to link the electrical output to the mechanical shape and the operational mode. Another method for representing piezoelectric harvesters is the distributed parameters of the electromechanical equation [6]. In this method the linear constitutive equation and the Rayleigh-Ritz solution are developed. Moreover, because the air tamping and the base motion which includes a small rotation are taken into account the electromechanical modeling for cantilever piezoelectric unimorph beam has its base on Euler-Bernoulli theory. Appropriate equivalent electrical circuitry of the cantilevered piezoelectric system is also developed [7] as the SPICE based software is introduced to represent the circuit connections. The advantage when using the simulation software is that it can easily capture the model behavior of each of the vibration modes. Other approaches of modeling which have their base on finite element method [8] are also researched as a means for derivation of the electromechanical coupled system equation for the piezoelectric cantilever beam utilizing finite element software package which is combined with SPICE simulation software for the electrical circuit. The dynamic behavior for power harvesting using finite element ANSYS (FEA) software package and equivalent circuit analysis using SPICE software are also in the development process [9]. The finite element procedure is proposed to find the static capacitance of the coupled structure, short-circuit resonance, charge response for each mode and determining all parameters found in the FEA software package for the SPICE circuit modeling. An array of piezoelectric harvesters (multiple identical harvesters are mounted on the same base) is presented by some researchers as a way to increase power output that can be harvested. The array application can result in the difficulties in finding the appropriate load for the device as the authors [10] are proposing the usage of the impedance for investigating the electrical response of the array. The current paper proposes a Multisim-based model of piezoelectric energy harvester.

2 FEATURES OF THE MULTISIM-BASED MODEL

A simple structure of a unimorph harvester is shown in Fig. 1. The harvester beam is supposed to be created when its base shows a motion.
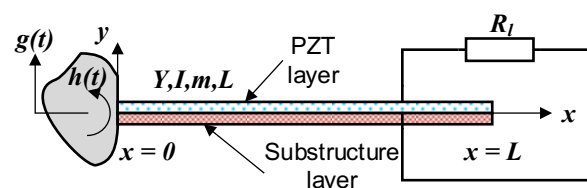

Fig. 1. Translational and small rotational base motion in a unimorph piezoelectric energy harvester

3. Modeling Assumptions

Simulation model

For the study of a unimorph piezoelectric energy harvester, the present work uses the Multisim-based model, proposed in [11]. The model is shown in Fig. 2.
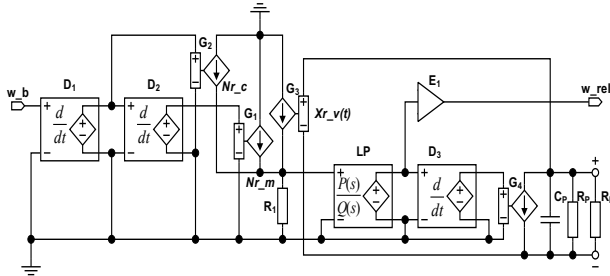

Fig. 2. Multisim model of a piezoelectric unimorph cantilever harvester

Multisim-based model in fig. 1 contains in its structure three differentiator blocks (D1÷D3), four gyrators (G1÷G4), one Laplace block (LP), one gain block (E1), a capacitance (Cp) and a resistance (Rp) of a piezoceramic layer. RL is the load resistance [9].

The gyrators are assumed as Voltage Controlled Current Sources (VCCS) and the block E1 as a two-pin voltage controlled voltage source (VCVS). The main reason is to validate the results obtained using the proposed Multisim model. Only the value of the resistivity is taken from [12]. The summary of the geometries and the material properties is given.

Frequency Range

To obtain the characteristics of the harvester in the frequency domain, it is required to set the frequency range. Knowing the frequency range allows determining the number and values of natural (or resonant) frequencies [2]. Therefore, three vibration modes can be studied in the specified frequency range.

Model Parameter Values

The calculated model parameter values for the first three vibration modes are listed in Table 1.

4 Simulation Results

Using the model parameters, given in Table 1, a parametric case simulation study for the unimorph energy harvester is performed. Single-mode and multi-mode FRFs of the voltage output are obtained.

$$Voltage\ FRF = \frac{v(t)}{-\omega^2 Y_0 e^{j\omega t}} \qquad (1)$$

The multi-mode FRF is obtained by summation of the single-mode FRFs, i.e.

$$FRF = \sum_{r=1}^{\infty}(FRF)_r \qquad (2)$$

where $(FRF)_r$ is the FRF of the r-th vibration mode.

The multi-mode voltage FRFs (per base acceleration) for various resistive load values over the frequency range of 0 – 1000 Hz are shown in Fig. 3. Represented here voltage frequency responses are based on the single-modes simulation results. The set of the electrical load resistance
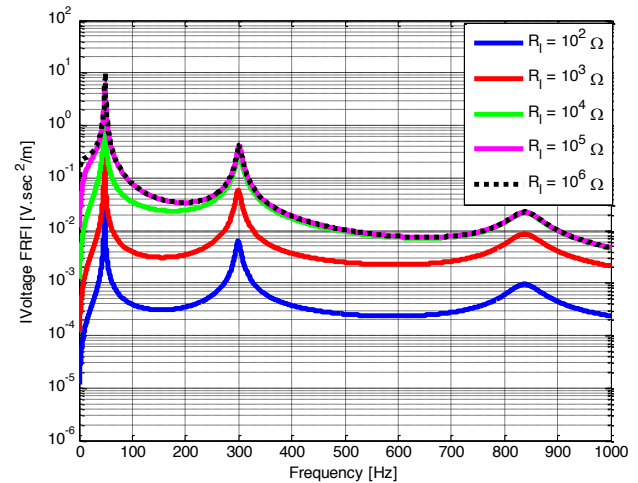
considered here ranges from 100 Ω to 1 MΩ.

Fig. 3. Three vibration modes are clearly visible for the defined frequency range (0-1000 Hz).

By changing the load from 100 , to 1M , the resonance frequency changes from 47.8 Hz to 48.8 Hz for the first Ω Ω [13] mode, from 299.6 Hz to 301.5 Hz for the second mode, and from 838.9 Hz to 839.9 Hz for the third [13] mode.

These three separate single mode representations (for mode 1, mode 2 and mode 3 independently) are approximately valid around the respective resonance frequencies only. Therefore, they are shown namely around these frequencies.

It follows from the simulated results for the first and second mode (Fig. 4 (a), (b)), that the voltage FRFs of the largest two values of load resistance are almost indifferent especially for the second mode, implying a convergence of the curves to the open-circuit voltage. From Fig. 4 (c), it can be seen that for the third vibration mode the voltage frequency response curve, of even 10 kΩ value of load resistance, coincides with the respective open-circuit curve. For a different configuration, it might be the case that even a load of 100 k might be sufficient to represent the open-circuit conditions.
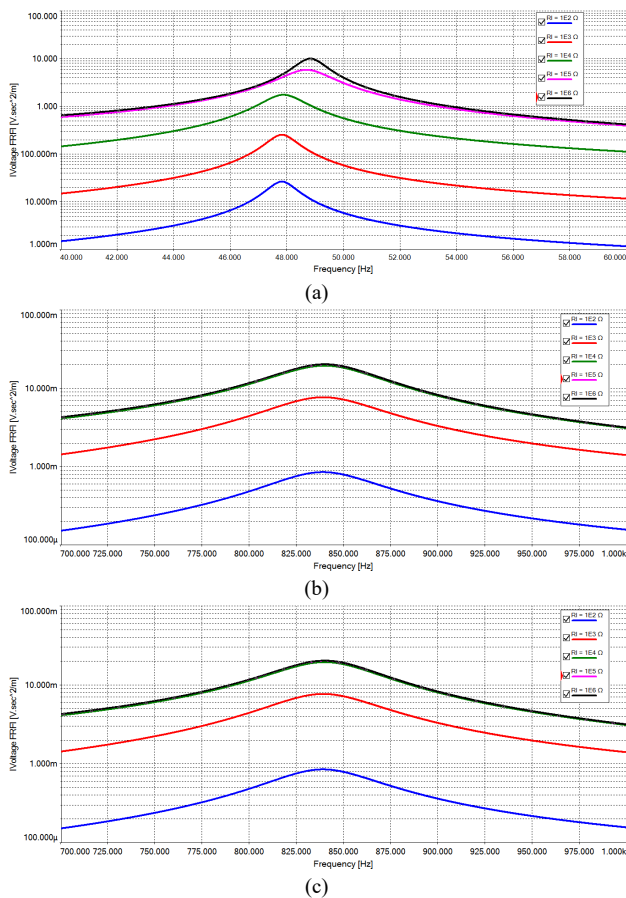
From the qualitative point of view, it is found that when the resistive load increases from 100 Ω to 1 MΩ, the maximum voltage output increases from 26.365 mV.sec^2/m (at 47.8 Hz) to 9.981 V.sec^2/m (at 48.8 Hz) for the first mode, from 6.213 mV.sec^2/m (at 299.6 Hz) to 413.486 mV.sec^2/m (at 301.5 Hz) for the second mode, and from 0.845 μV.sec^2/m (at 838.9 Hz) to 20.158 mV.sec^2/m (at 839.9 Hz) for the third mode, respectively.

For the so found intersection point, that is, for a load resistance of 40.07 kΩ, the voltage response has the same amplitude (3.305 V.sec2/m) for excitations at both frequencies. The maximum voltage amplitude limit $R_l = \infty$ actually, $R_l = 1MΩ$) is about 4.594 V.sec^2/m for excitation at 47.8 Hz and it is about 9.981 V.sec^2/m for excitation at 48.8 Hz.

The obtained simulation results for voltage FRFs have a good agreement with the analytical results in [12]. The existing insignificant difference in results obtained using the Multisim-based model and analytical model can be due to the discretization errors within the Multisim solver and rounding errors from the pre-calculated modal parameters.

Table 1: Blocks/elements settings for the first three vibration modes

Block/ Element	Parameter Value		
	Mode 1	Mode 2	Mode 3
G1	-0.090769	-0.050241	-0.029457
G2	0.442941	0.245479	0.143929
G3	0.017563	-0.060997	0.100140
G4	0.017563	-0.060997	0.100140
LP	$\dfrac{1}{s^2 + 6.007883s + 9.023663e4}$	$\dfrac{1}{s^2 + 48.9459853s + 3.543949e6}$	$\dfrac{1}{s^2 + 3.478966e02s + 2.778513e07}$
E	17.274146	-17.274146	17.274146
D1, D2, D3	1		
R_p	0.200 TΩ		
C_p	79.650 pF		

(a)

(b)

(c)

Fig. 4. Voltage FRFs of the first three vibration modes for five different values of load resistance
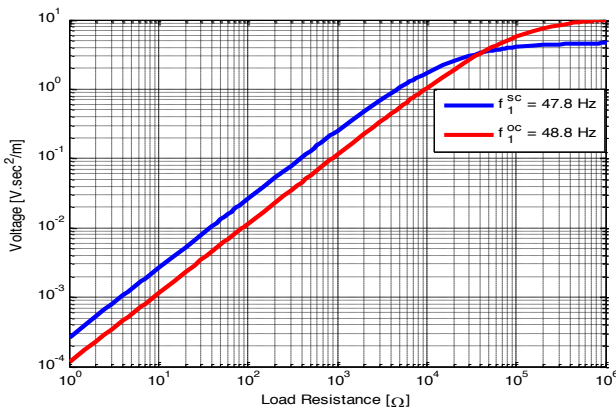
Fig. 5. The maximum voltage amplitude in the limit $R_l = \infty$ actually, $R_l = 1MΩ$

The input displacement is fed to the input of the differentiator block **D1**, which gives the first derivative of the $w_b(t)$ i.e., the velocity of the mounting base (which is $j\omega Y_0 e^{j\omega t}$). The second derivative of the $w_b(t)$– the acceleration of the base ($-\omega^2 Y_0 e^{j\omega t}$), is obtained at the output of the differentiator block **D2**. The model contains four gyrators (**G1 ÷ G4**) a search gyrator is represented by Voltage Controlled Current Source (VCCS). Gyrators **G1** and **G2** convert the acceleration and velocity of the base to components of mechanical excitation with $h(t) = 0$. The two components of mechanical excitation (N_r^m and N_r^c) are, respectively, marked as **Nr_m** and **Nr_c**. The force contribution from the applied/induced voltage in the piezoelectric layer is modeled by gyrator **G3** and is marked as **Xr_v(t).**The feedback from the electrical to mechanical system is modeled using the gyrator **G3**.The components **Nr_m** and **Nr_c** are summed and the force **Xr_v(t)** is subtracted from the result, applying Kirchhoff's law with a **1** ohm resistor (resistorR_l) to ground. In this way, the right-hand side of the modal equation (15) is obtained, which is solved by the Laplace block **LP** that gives the modal amplitude $\eta(t)$. The differentiator block **D3** is used to obtain the first derivative of the modal mechanical function.

Determining the Model Parameters
Each block/element of the model requires a specific parameter to be predetermined. The model parameters are summarized in Table 2. For calculating the values of the model parameters, using Matlab software [15], a suitable code has been written. In order to obtain the parameter values for numerous vibration modes without repeating some operations, in this code symbolic variables are used. Moreover, the eigenfunction $\phi_r(x)$ is also specified as a symbolic function. In this case, the symbolic differentiation and symbolic integration of the function $\phi_r(x)$ can be performed. As a result, the first derivative $d\phi_r(x)/dx$ and the integral $\int_{x=0}^{L} \phi_r(x)dx$ are also obtained as symbolic functions.

Once obtained, the symbolic expressions can be repeatedly used for calculation for specific values for different vibration modes. The damping ratios ζ_1 and ζ_2 of the first two modes are supposed to be recognized as well.

The model parameters are calculated and a vibration mode should be chosen. The first mode is ought to be chosen due to its dominating influence over the output. The r-th solution of the characteristic equation corresponds to the r-th vibration mode. Solving the characteristic equation requires for each root to be defined either the initial approximation or

the interval in which the root is located. As the roots are considered to be points where the function actually crosses, not just touches, the x-axis, the easiest and precise way to fix the initial roots approximation or the intervals in which the function changes its sign, is to display the function graphically. This approach is used here to solve for λ_r. The values of $\phi_r(L)$, $d\phi_r(L)/dx$ and $\int_0^L \phi_r(x)dx$ can be calculated using respective symbolic expressions, when knowing the value of λ_r for the r-th vibration mode as well as the harvester parameters. The value of the undamped natural frequency ω_r and of the modal coupling terms χ_r and k_r for the r-th mode is determined. In other words, the proportional damping coefficients c_sI and c_a can be defined by using the ω_r and ζ_r parameters for the first and second modes (that is, for $r = 1$ and $r = 2$).

$$\begin{bmatrix} c_S I \\ c_a \end{bmatrix} = \frac{2\omega_j\omega_k}{\omega_j^2 - \omega_k^2} \begin{bmatrix} \dfrac{YI}{\omega_k} & -\dfrac{YI}{\omega_j} \\ -m\omega_k & m\omega_j \end{bmatrix} \begin{bmatrix} \zeta_j \\ \zeta_k \end{bmatrix} \tag{3}$$

Finally, the values for the coefficients $m\gamma_r^w$ and $c_a\gamma_r^w$, required to obtain the components of mechanical excitation, as well as for the coefficients $2\zeta_r\omega_r$ and ω_r^2 of the left side of the modal motion equation are calculated.

Table 2. Parameters of the model blocks/elements

Block/Element	Label	Model Parameter – Value/Expression
Differentiator	D1	1
	D2	1
	D3	1
Gyrator	G1	$-m\int_{x=0}^{L} \phi_r(x)dx$
	G2	$-c_\alpha\int_{x=0}^{L} \phi_r(x)dx$
	G3	$-k_r$
	G4	$-\chi_r$
Laplace function	LP	$1/(s^2 + 2\zeta_r\omega_r s + \omega_r^2)$
Gain_2_PIN	E₁	$\phi_r(L)$
Resistance	R₁	1Ω
Internal resistance of the PZT layer	Rₚ	$\rho_p \dfrac{h_p}{bL}$
Internal capacitance of the PZT layer	Cₚ	$\dfrac{\varepsilon_{33}^S bL}{h_p}$

The flow diagram of the steps required to calculate parameters used by Multisim-based model, is shown in Fig. 6.
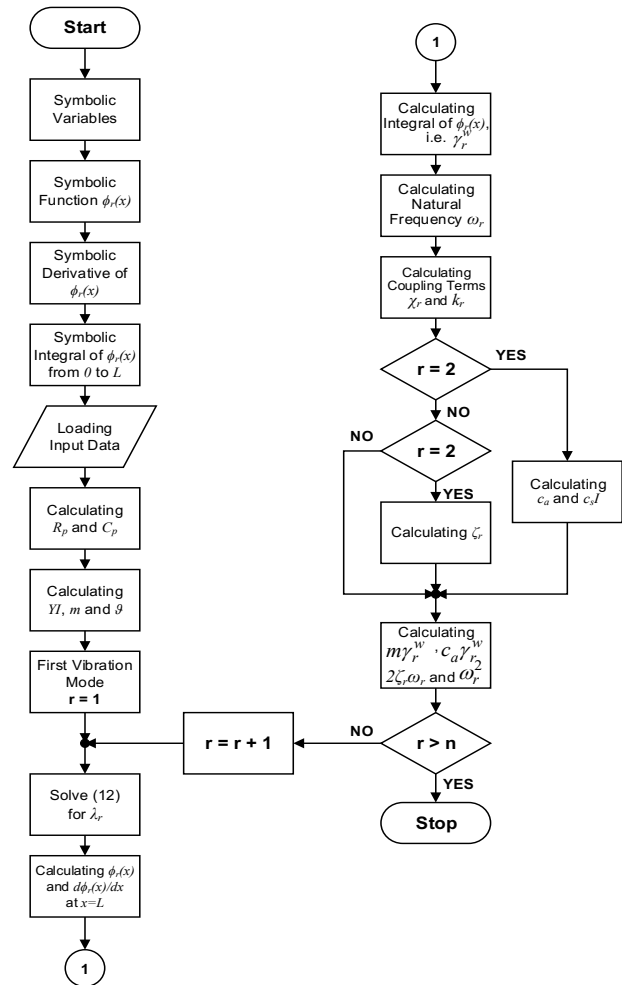
Fig. 6. Flowchart for obtaining the model parameters

5 Conclusions

In this paper, a simulation study for a specified unimorph piezoelectric energy harvester is performed by using a Multisim-based model. Also a modeling procedure using Euler-Bernoulli beam theory as well a procedure for obtaining the model parameters are described. The Multisim model and the proposed approach for results processing can be successfully applied to studies in regard to the frequency responses of such electrical outputs in energy harvesters.

References

1. Hristov I, Goran GORANOV, and Radoslava Hristova, Nonlinear Wave Simulation on the Xeon Phi Knights Landing Processor. EPJ Web MMCP, Volume 173, 2018 Dubna Russia. ISSN:2100-014X.A.
2. Sodano H. A., D. J. Inman, G. Park. Generation and storage of electricity from power harvesting devices. Journal of Intelligent Material Systems and Structures, 2005, 16(1), 67-75.
3. Chen S.-N., G.-J. Wang, M.-C. Chien. Analytical modeling of piezoelectric vibration-induced micro power generator. Mechatronics, 2006, 16(7), 379-387.
4. Erturk A., D. J. Inman. On Mechanical Modeling of Cantilevered Piezoelectric Vibration Energy Harvesters. Journal of Intelligent Material Systems and Structures, vol. 19, no. 11, pp. 1311-1325, 2008.
5. Lu F., H. P. Lee, S. P. Lim. Modeling and Analysis of Micro Piezoelectric Power Generators for Micro-Electromechanical-

Systems Applications. Smart Materials and Structures, 13, pp. 57-63, 2004.

6. Erturk A., D. J. Inman. A distributed parameter electromechanical model for cantilevered piezoelectric energy harvesters. Journal of Vibration and Acoustics, 2008, 130(4), 041002.

7. Elvin N. G., A. A. Elvin. A general equivalent circuit model for piezoelectric generators. Journal of Intelligent Material Systems and Structures, 2009, 20(1), 3-9.

8. Elvin N. G., A. A. Elvin. A coupled finite element—circuit simulation model for analyzing piezoelectric energy generators. Journal of Intelligent Material Systems and Structures, 2009, 20(5), 587-595.

9. Yang Y., L. Tang. Equivalent circuit modeling of piezoelectric energy harvesters. Journal of Intelligent Material Systems and Structures, 2009, 20 (18), 2223-2235.

10. Lien I., Y. Shu. Array of piezoelectric energy harvesting by the equivalent impedance approach. Smart Materials and Structures, 2012, 21(8), 082001.

11. Xiong X., S. O. Oyadiji. Modal electromechanical optimization of cantilevered piezoelectric vibration energy harvesters by geometric variation. Journal of Intelligent Material Systems and Structures, 2013, 1045389X13502872.

12. Lumentut M., I. Howard. Electromechanical finite element modeling for dynamic analysis of a cantilevered piezoelectric energy harvester with tip mass offset under base excitations. Smart Materials and Structures, 2014, 23(9), 095037.

13. Inman D. J. Engineering Vibration. Prentice Hall, Englewood Cliffs, New Jersey, 2007.

14. duToit N. E., B. L. Wardle, S. Kim. Design Consideration for MEMS-Scale Piezoelectric Mechanical Vibration Energy Harvesters. Integrated Ferroelectrics, 71, pp. 121-160, doi:10.1080/10584580590964574.

15. The MathWorks, Inc. http://www.mathworks.com